



Regenerative potential of adipocytes in hypertrophic scars is mediated by myofibroblast reprogramming

Katharina Hoerst¹ · Lenie van den Broek² · Christoph Sachse³ · Oliver Klein⁴ · Uwe von Fritschen⁵ · Sue Gibbs² · Sarah Hedtrich^{1,6} 

Received: 5 November 2018 / Revised: 6 March 2019 / Accepted: 8 March 2019 / Published online: 19 March 2019
© Springer-Verlag GmbH Germany, part of Springer Nature 2019

Abstract

Abnormal scarring is a major challenge in modern medicine. The central role of myofibroblasts and TGF- β signaling in scarring is widely accepted, but effective treatment options are missing. Autologous fat grafting is a novel approach that has led to significant improvements in the functionality and appearance of scar tissue. While the underlying mechanism is unknown, the potential role of paracrine effects of adipocytes has been discussed. Hence, with the aim of unraveling the regenerative potential of adipocytes, their effects on in vitro differentiated myofibroblasts and on fibroblasts from hypertrophic scars were investigated. Exposure to adipocyte-conditioned medium significantly decreased the expression of the myofibroblast marker α -SMA and ECM components, indicating the occurrence of myofibroblast reprogramming. Further analysis demonstrated that myofibroblast reprogramming was triggered by BMP-4 and activation of PPAR γ signaling initiating tissue remodeling. These findings may pave the way for novel therapeutic strategies for the prevention or treatment of hypertrophic scars.

Key messages

- Adipocytes induce distinct regenerative effects in hypertrophic scar tissue.
- Adipocytes secrete several proteins which are involved in wound healing and regeneration.
- Adipocytes secrete BMP-4 which activates myofibroblast reprogramming.
- Mediators secreted by adipocytes directly and indirectly activate PPAR γ which exerts distinct anti-fibrotic effects.
- These findings may pave the way for novel therapeutic strategies for the prevention or treatment of hypertrophic scars.

Keywords Myofibroblast · Wound healing · Hypertrophic scar · Adipocyte · Bone morphogenetic protein

Electronic supplementary material The online version of this article (<https://doi.org/10.1007/s00109-019-01772-2>) contains supplementary material, which is available to authorized users.

✉ Sarah Hedtrich
sarah.hedtrich@ubc.ca

¹ Institute of Pharmaceutical Sciences, Pharmacology and Toxicology, Freie Universität Berlin, 14195 Berlin, Germany

² Department of Dermatology, VU University Medical Center, 1081, HV Amsterdam, The Netherlands

³ NMI TT Pharmaservices, 13353 Berlin, Germany

⁴ Charité-Universitätsmedizin Berlin, Corporate Member of Freie Universität Berlin, Humboldt-Universität zu Berlin, and Berlin Institute of Health, 13353 Berlin, Germany

⁵ Division of Plastic Surgery and Hand Surgery, Helios Clinic, 14165 Berlin, Germany

⁶ University of British Columbia, Faculty of Pharmaceutical Sciences, Vancouver, Canada

Introduction

Abnormal scarring and its accompanying cosmetic, functional, and psychological burden is a major challenge in modern medicine. Up to 30% of elective surgeries are followed by aberrations in physiological wound healing, resulting in hypertrophic scarring or keloid formation [1].

One of the most prominent cell types involved in normal and pathological tissue repair are myofibroblasts, which are alpha-smooth muscle actin (α -SMA)-positive cells that deposit extracellular matrix (ECM) proteins, such as collagen 1 and 3. Activated by transforming growth factor (TGF)- β 1, myofibroblasts exhibit a contractile phenotype, thereby promoting wound closure. In physiological processes, myofibroblasts normally undergo apoptosis when the re-epithelization phase is initiated [2]. Under pathological conditions, myofibroblasts accumulate, and ECM deposition is excessive and occurs continuously, ultimately leading to scar formation [3]. Myofibroblasts have long been considered to be terminally differentiated cells; however, evidence has accumulated showing that myofibroblast re- or dedifferentiation is possible [4–6]. Given that myofibroblast appearance and dysfunction has severe consequences, knowledge about their development, function, and survival is crucial to find preventive or therapeutic approaches for scar tissue. A relatively new treatment option for hypertrophic scars is autologous fat grafting, resulting in partial but significant improvements in the functionality and appearance of scar tissue [7]. However, the underlying mechanisms are still ambiguous, but the paracrine effects of adipocytes are being discussed. Adipose tissue is a highly complex organ composed of several cell types, including adipocytes, various types of immune cells, and mesenchymal stem cells (adipose-derived stem cells; ASCs). ASCs are multipotent precursor cells that are able to differentiate into chondrocytes, osteoblasts, or adipocytes [8] and have been extensively investigated for their regenerative potential [9, 10]. In contrast, little is known about the regenerative potential of adipocytes, which are highly active secretory cells that release hundreds of different factors involved in various (patho-)physiological processes [11, 12]. Nevertheless, an antagonistic relationship between peroxisome proliferator-activated receptor gamma (PPAR γ), a master regulator of adipogenesis, and TGF- β signaling has been repeatedly demonstrated [13–15].

To elucidate the regenerative effects of adipocytes, we studied the crosstalk between in vitro differentiated adipocytes (in this study further referred to adipocytes) and TGF- β -induced myofibroblasts as well as fibroblasts isolated from hypertrophic scars and, for specific investigations, from keloids. Following incubation of myofibroblasts or fibroblasts isolated from hypertrophic scars with adipocyte-conditioned medium (CM), the expression of characteristic myofibroblast markers was analyzed. Furthermore, specific inhibitor assays

and high-throughput protein expression analyses were performed to obtain a more detailed understanding of the downstream effects on intracellular signaling.

Materials and methods

Contact for reagent and resource sharing

Further information and requests for resources and reagents should be directed to and will be fulfilled by the Lead Contact, Sarah Hedtrich (sarah.hedtrich@ubc.ca).

Experimental model and subject details

Primary human fibroblasts were isolated from juvenile foreskin following circumcision (approved by the ethics committee of the Charité–Universitätsmedizin Berlin, Germany, EA1/081/13, informed consent was obtained from parents/LAR) according to standard procedures. Fibroblasts were cultivated in Dulbecco's modified Eagle's medium (DMEM, Sigma-Aldrich, Munich, Germany) supplemented with 7.5% FBS, 2 mM L-glutamine, 100 units/ml penicillin, and 100 μ g/mL streptomycin. Cultures were maintained at 37 °C in a humidified atmosphere containing 5% CO₂. For every experiment, cells (passage 2–3) from three different donors were pooled. To generate myofibroblasts, fibroblasts were serum-starved for 72 h followed by 96 h of stimulation with 10 ng/ml TGF- β 1 (Miltenyi Biotec, Bergisch-Gladbach, Germany).

Hypertrophic scars and keloid fibroblasts were obtained from patients undergoing scar removal via excision. The discarded scar tissue was used in anonymous fashion in compliance with the VU University Medical Center's ethical guidelines and the "Code for Proper Use of Human Tissues" as formulated by the Dutch Federation of Medical Scientific Organizations (see www.fmwv.nl). Cultures were maintained in DMEM, containing 7.5% FBS, 100 units/ml penicillin, and 100 μ g/mL streptomycin and used for experiments in passages 2–3.

Adipose-derived stem cells (ASCs) were isolated from adipose tissue obtained from breast reconstruction and abdominal plastic surgeries in Caucasian patients (approved by the ethics committee of the Charité–Universitätsmedizin Berlin, Germany, EA2/121/15, with patient's consent). Briefly, adipose tissue was washed in PBS, minced, and incubated with collagenase mix (1 mg/ml collagenase I, 4% BSA, 1% penicillin/streptomycin) for 50 min at 37 °C. Cell suspension was then passed through 100- μ m and 70- μ m strainers, centrifuged (300 \times g, 5 min) and seeded in DMEM/F12 (Sigma-Aldrich, Munich, Germany) supplemented with 10% FBS, 100 units/ml penicillin, and 100 μ g/mL streptomycin. To induce adipogenesis, ASCs (passage 2–3) were further cultivated in DMEM/F12 supplemented with 10% FBS, 10 μ g/mL insulin,

1 μ M dexamethasone (Sigma-Aldrich, Munich, Germany), 0.5 mM IBMX (Life Technologies, Darmstadt, Germany), and 1% penicillin/streptomycin for 14 days.

Method details

Trilineage differentiation of ASCs

ASCs were subjected to the adipogenic differentiation (see details above) cocktail for 14 days. To verify the presence of in vitro differentiated adipocytes, lipid droplets were visualized by Oil Red O staining as follows. The cells were washed with PBS followed by fixation in 4% PFA for 10 min (Carl Roth, Karlsruhe, Germany). After another washing step, the cells were incubated in 0.5% Oil Red O staining solution for 30 min. Cells were then washed in water until staining solution was removed and imaged with a phase contrast microscope (Axiovert 135, Carl Zeiss, Jena, Germany).

Osteogenesis was induced by cultivating ASCs for 14 days in differentiation medium containing 10% FBS, 0.1 μ M dexamethasone, 50 μ M ascorbate-2-phosphate, and 10 mM β -glycerophosphate (Sigma-Aldrich, Munich, Germany). Successful differentiation was verified by Alizarin Red staining (Sigma-Aldrich, Munich, Germany). Cells were washed, fixed, and incubated with 40 mM Alizarin Red staining solution for 20 min. Following washing, cells were imaged with a phase contrast microscope.

For chondrogenic induction, ASCs were cultivated using a micromass technique. Micromasses were obtained by pipetting 10 μ l of cell suspension containing 100,000 ASCs into wells of a 6-well-plate. After 2 h, growth medium was added. Then, 24 h later, the culture medium was changed to chondrogenic differentiation medium containing 1% FBS, 6.25 μ g/mL insulin, 10 ng/mL TGF- β 1, and 50 nM ascorbate-2-phosphate. After 14 days, chondrogenic differentiation was verified by Alcian Blue staining (Sigma-Aldrich, Munich, Germany).

Conditioned medium preparation

To obtain conditioned medium (CM) from ASCs and adipocytes (passage 2–3), cells were cultivated as described previously. To obtain CM, ASC and adipocyte culture media were replaced with serum-free media for 24 h to avoid FBS contamination. Subsequently, CM was collected, centrifuged, and filtered using 0.45- μ m filters (Sarstedt, Nürnbrecht, Germany).

Incubation with conditioned medium

Myofibroblasts or fibroblasts isolated from hypertrophic scars were washed twice with PBS and then incubated with CM

from either ASCs or adipocytes for 24 h. Myofibroblasts cultured in standard serum-free medium served as the control.

Inhibition studies were performed with the PPAR γ inhibitor GW9662 (1 μ M; Sigma-Aldrich, Munich, Germany) or the BMP receptor type I antagonist LDN-193189 (200 nM; Sigma-Aldrich, Munich, Germany). Myofibroblasts and hypertrophic scar fibroblasts were pretreated with either 1 μ M GW9662 or 200 nM LDN-193189 for 30 min followed by 24 h incubation with CM. Cells cultured in serum-free medium served as the control.

Western blot

Cells were lysed in radioimmunoprecipitation assay buffer for 30 min on ice followed by centrifugation (13,000 \times g, 30 min, 4 $^{\circ}$ C). Protein concentration was calculated using a Pierce $\text{\textcircled{R}}$ BCA Protein Assay Kit (Thermo Scientific). Subsequently, 20 μ g of protein lysate was diluted in standard SDS-PAGE sample buffer supplemented with 100 mM DTT, boiled at 95 $^{\circ}$ C, and subjected to SDS-PAGE. After transfer of the protein onto nitrocellulose membranes (Bio-Rad, Munich, Germany) using a semi-dry transfer system (Bio-Rad, Munich, Germany), the membranes were blocked in Tris-buffered saline containing 0.1% Tween-20 (TBST, Sigma-Aldrich, Munich, Germany) supplemented with 5% skimmed milk powder or 5% BSA for 1 h at room temperature. The membranes were further incubated with primary antibodies diluted 1:1000 in TBST with 5% skimmed milk at 4 $^{\circ}$ C overnight. After the membranes were washed in TBST, anti-rabbit or anti-mouse horseradish peroxidase-conjugated secondary antibodies were applied for 1 h at room temperature. The blots were washed again, developed using SignalFire TM ECL reagent (Cell Signaling Technology, Frankfurt/Main, Germany), and visualized with a PXi/PXi Touch gel imaging system (Syngene, Cambridge, UK). Immunoblotting quantification was performed using ImageJ software (Version 1.46r, National Institute of Health, MD, USA). ImageJ was applied to analyze protein expression via densitometry. Target protein intensity was compared to that of the loading control (β -Actin or β -Tubulin). A list of the primary and secondary antibodies used can be found in Table S2.

Cellular subfractionation

To separate the nuclear and cytoplasmic fractions of myofibroblasts, a NE-PER Nuclear and Cytoplasmic Extraction Reagents Kit (Thermo Fisher Scientific, Schwerte, Germany) was used. Prior to cellular subfractionation, myofibroblasts were stimulated with adipocyte-CM for 24 h or maintained in serum-free medium (control). Subsequently, the cells were trypsinized and centrifuged (500 \times g, 3 min), and the cell pellets were further processed according to the manufacturer's instructions.

Enzyme-linked immunosorbent assay (ELISA)

To quantify BMP concentrations in CM from ASCs and adipocytes, ELISAs were performed using human BMP 2, 4, 6, and 7 ELISA Kits (Thermo Fisher Scientific, Schwerte, Germany) according to the manufacturer's instructions. Samples were measured in duplicates.

DigiWest[®] multiplexed protein profiling

Myofibroblasts were stimulated with adipocyte-CM or serum-free medium for 24 h. Subsequently, cells were washed twice in ice-cold PBS, detached, and then centrifuged at 4 °C (2 min, 13,000×g). The DigiWest[®] protein profiling procedure was performed as described previously [16]. Briefly, SDS-PAGE and Western blotting onto PVDF membranes was performed using the NuPAGE system (Life Technologies, Darmstadt, Germany). Blots were washed in PBS containing 0.1% Tween-20 (PBST). The proteins were biotinylated on the membrane using NHS-PEG12-Biotin in PBST and then washed in PBST and dried. Each sample lane was sliced into 96 fractions of 0.5 mm each, and the proteins were eluted in 96-well plates using elution buffer (8 M urea, 1% Triton-X 100 in 100 mM Tris-HCl, pH 9.5). The eluted proteins from each molecular weight fraction were loaded onto one distinct color of neutravidin-coated MagPlex beads (Luminex Corporation, Texas, USA) and pooled afterwards. A total of 10 µg of protein per cell sample was used for 96 different antibody incubations. Aliquots of the DigiWest[®] bead mixes were added to 96-well plates containing assay buffer (Blocking Reagent for ELISA (Roche, Penzberg, Germany)) supplemented with 0.2% milk powder, 0.05% Tween-20, and 0.02% sodium azide. After the assay buffer was discarded, diluted primary antibodies were added (see Table S3). Following overnight incubation, bead mixes were washed twice with PBST, and phycoerythrin-labeled diluted secondary antibodies were added. Beads were washed twice, and assay results were measured on a Luminex FlexMAP 3D system. Antibody-specific signals were quantified using the DigiWest[®] data analysis tool to identify the peaks of correct molecular weight and to calculate peak areas. For comparative analyses between the samples, protein expression values were normalized to the total protein amount.

Mass spectrometry

Liquid chromatography/electron spray ionization mass spectrometry (LC/ESI-MS) was performed as described previously [17]. Briefly, 1 ml of CM from three independent donors (A, B, C) was rebuffed in Amicon[®] Ultra centrifugal filters with 0.11 mM CHAPS (0.05 M Tris-HCl (pH 7.5)/0.05 M KCl, 20% glycerin), 8 M urea/0.1 M/Tris-HCl (pH 8.5), and 50 mM ammonium bicarbonate (ABC, Sigma-Aldrich, Munich, Germany) to a final volume of 40 µl. Subsequently, 50 µl

of 0.2 µg/µL trypsin (Promega, Mannheim, Germany) in 50 mM ABC was added and incubated with the sample overnight at 37 °C. Peptides were extracted with 60 µl of 0.1% TFA and directly analyzed by LC/ESI-MS. Peptide separation was performed (2–60% acetonitrile/in 0.1% formic acid, flow rate 400 nl/min) using an analytical UHPLC system (Dionex Ultimate 3000 RSLC, Thermo-Fisher, Waltham, MA, USA) and analyzed with an ESI-QTOF mass spectrometer (Impact II, Bruker Daltonics, Billerica, MA, USA). Mass spectra were evaluated using MASCOT software (version number 2.2, Matrix Science, Boston, MA, USA) by automatically searching the SwissProt 51.9 database (553474 sequences; 198069095 residues, Cambridgeshire, UK). The MS/MS ion search was performed with the following set of parameters: (i) taxonomy, *Homo sapiens* (human) (20172 sequences); (ii) proteolytic enzyme, trypsin; (iii) maximum of accepted missed cleavages, 2; (iv) mass value, monoisotopic; (v) peptide mass tolerance, 10 ppm; (vi) fragment mass tolerance, 0.05 Da; and (vii) variable modifications, oxidation of methionine. Only proteins with scores corresponding to $p < 0.05$ and with at least two independent peptides were considered. Visualization of protein interaction networks was performed with the String database using a high confidence interaction score (0.7) and experiments, databases, gene fusion, and neighborhood as active interaction sources. GO enrichment analysis was performed using the open access platform Term Finder with cellular component as the ontology aspect.

Statistical analysis

Statistical testing was performed using GraphPad Prism software (GraphPad Software, La Jolla, CA). The data from at least three independent experiments are presented as the means ± standard error of the mean (SEM). Significance was determined with a one-sample *t* test followed by Bonferroni correction for multiple testing; * $p \leq 0.05$ and ** $p \leq 0.01$. Each sample (CM ASC or CM adipocytes) was tested against the control but not against each other. For ELISA, one-way analysis of variance and Bonferroni post hoc test was performed.

Results

Secretome analysis of in vitro differentiated adipocytes shows secretion of ~ 290 mediators

First, liquid chromatography-based mass spectrometry shotgun proteomics approach demonstrated the secretion of 160 proteins from ASCs and 288 from in vitro differentiated adipocytes. A subsequent literature comparison revealed that 90 of the proteins are commonly identified in adipocyte-conditioned medium (CM; Fig. 1; Tables S1 and Table S4)

[18–21]. Using a search tool for the retrieval of interacting genes and proteins, wound healing processes (GO: 0042060) were significant ($p \leq 0.01$) enriched and included 23 proteins. In addition, 5 of these proteins could be assigned to the GO term regeneration (GO: 0031099; Fig. 1 and Table S1).

α -SMA expression is significantly downregulated in TGF- β -induced myofibroblasts and hypertrophic scar fibroblasts following incubation with adipocyte-CM

ASC identity was confirmed by verifying the high expression of the mesenchymal surface markers CD34 and 105 and low CD45 (Fig. S1A) and by their potential of trilineage differentiation into

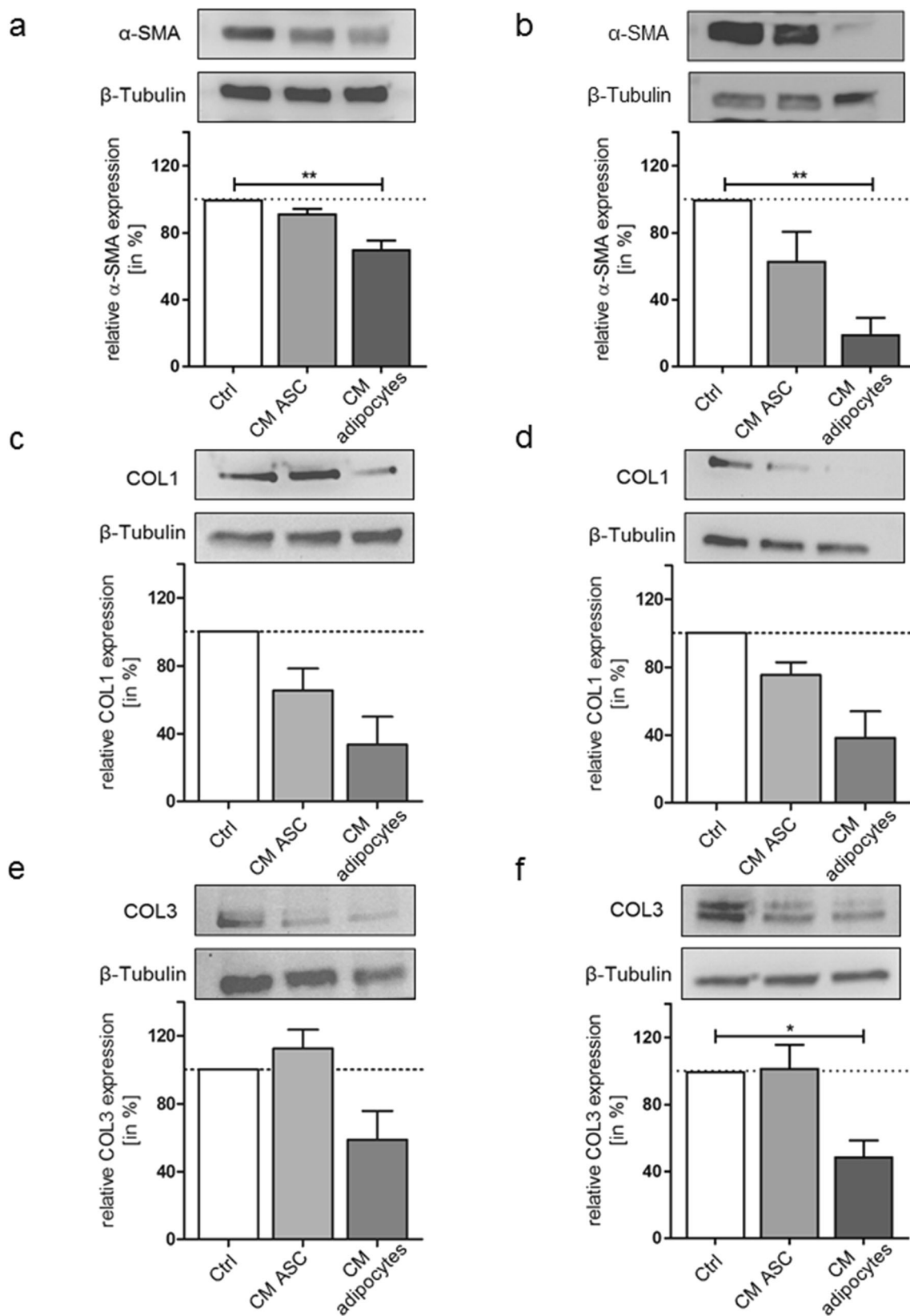
adipocytes, osteoblasts, and chondrocytes (Fig. S1B–D). Adipogenic differentiation of ASCs was verified by Oil Red O staining.

Subsequent incubation of myofibroblasts with adipocyte-CM for 24 h resulted in significantly reduced expression of the myofibroblast marker α -SMA ($-29.5\% \pm 4.9\%$; Fig. 2a). Further, a clear trend toward reduced deposition of the ECM components collagen 1 ($-66.4\% \pm 16.4\%$; Fig. 2c, $p = 0.056$) and collagen 3 ($-41.3\% \pm 17.1\%$; Fig. 2e, $p = 0.073$) was observed, indicating myofibroblast reprogramming. Notably, this effect was most pronounced in fibroblasts isolated from hypertrophic scars (Fig. 2b with $80.5\% \pm 9.6\%$; Fig. 2d with 61.7% , $p = 0.059$; Fig. 2f with $51.1\% \pm 9.6\%$). Incubation with ASC-CM resulted in less



Fig. 1 Secretome analysis of in vitro differentiated adipocytes shows secretion of 288 mediators. STRING analysis of the 90 out of 288 proteins that have been previously identified in the adipocyte secretome. Among these, 23 are associated with wound healing (red spheres) and 5 with regeneration (blue spheres) according to GO terms.

The lines indicate known protein interactions based on curated databases (turquoise), experiments (pink), predicted interactions for neighborhood (green), or gene fusion (red). Detailed information regarding the identified proteins is provided in Table S1



distinct effects. In addition, myofibroblast contraction was also reduced in the presence of adipocyte-CM whereas

myofibroblast migration and proliferation remained unaffected (Fig. S4).

Fig. 2 α -SMA expression is significantly downregulated in myofibroblasts and hypertrophic scar fibroblasts following incubation with adipocyte-CM. Representative Western blots and associated semi-quantification by densitometry showing the relative protein expression of α -smooth muscle actin (α -SMA), collagen 1 (COL1), and collagen 3 (COL3) in TGF- β -induced myofibroblasts (**a, c, e**) and hypertrophic scar fibroblasts (**b, d, f**) after exposure to conditioned medium (CM) from adipocytes and adipose-derived stem cells (ASCs). Ctrl = control, serum-free medium treatment. The data are presented as the mean \pm SEM; $n = 3-5$ (* $p \leq 0.05$ and ** $p \leq 0.01$)

Non-canonical TGF- β signaling elements are downregulated in myofibroblasts following incubation in CM

With the aim of investigating the underlying signaling, CM-treated TGF- β -induced myofibroblasts and hypertrophic scar fibroblasts were further analyzed for canonical and non-canonical TGF- β signaling elements. Whereas no significant alterations in phosphorylated SMAD 2/3 were observed (Fig. S2A), a significant decrease in phosphorylated extracellular signal-regulated kinase 1/2 (ERK 1/2)

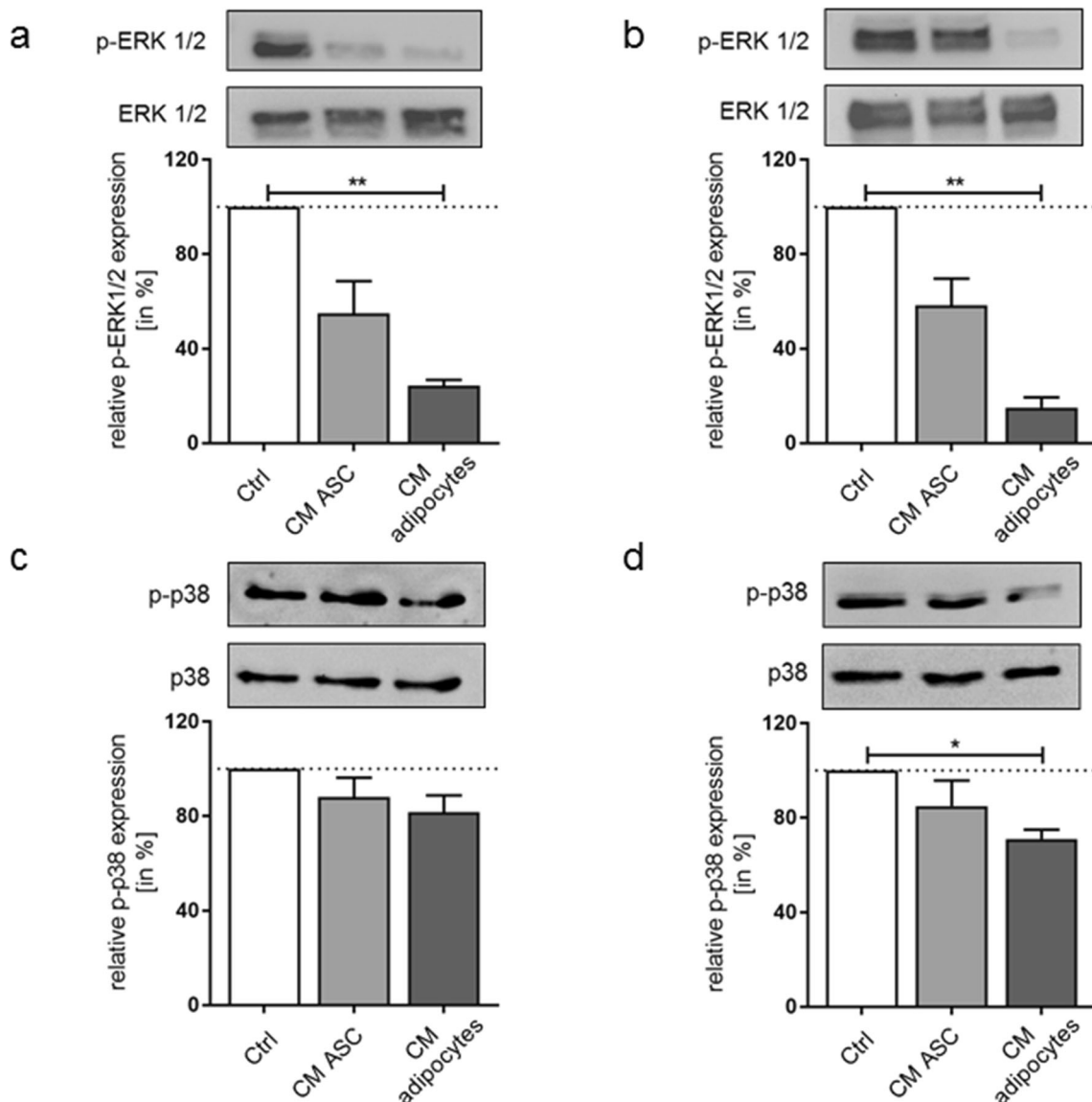


Fig. 3 Non-canonical TGF- β signaling elements are reduced in myofibroblasts following CM incubation. Representative Western blots and relative protein expression (semi-quantified by densitometry) of phosphorylated ERK 1/2 (p-ERK 1/2) and phosphorylated p38 (p-38) in TGF- β -induced myofibroblasts (**a, c**) and hypertrophic scar fibroblasts

(**b, d**) following incubation with CM from adipose-derived stem cells (ASCs) and adipocytes. Ctrl = control, serum-free medium treatment. The data are presented as the mean \pm SEM; $n = 3-5$ (* $p \leq 0.05$ and ** $p \leq 0.01$)

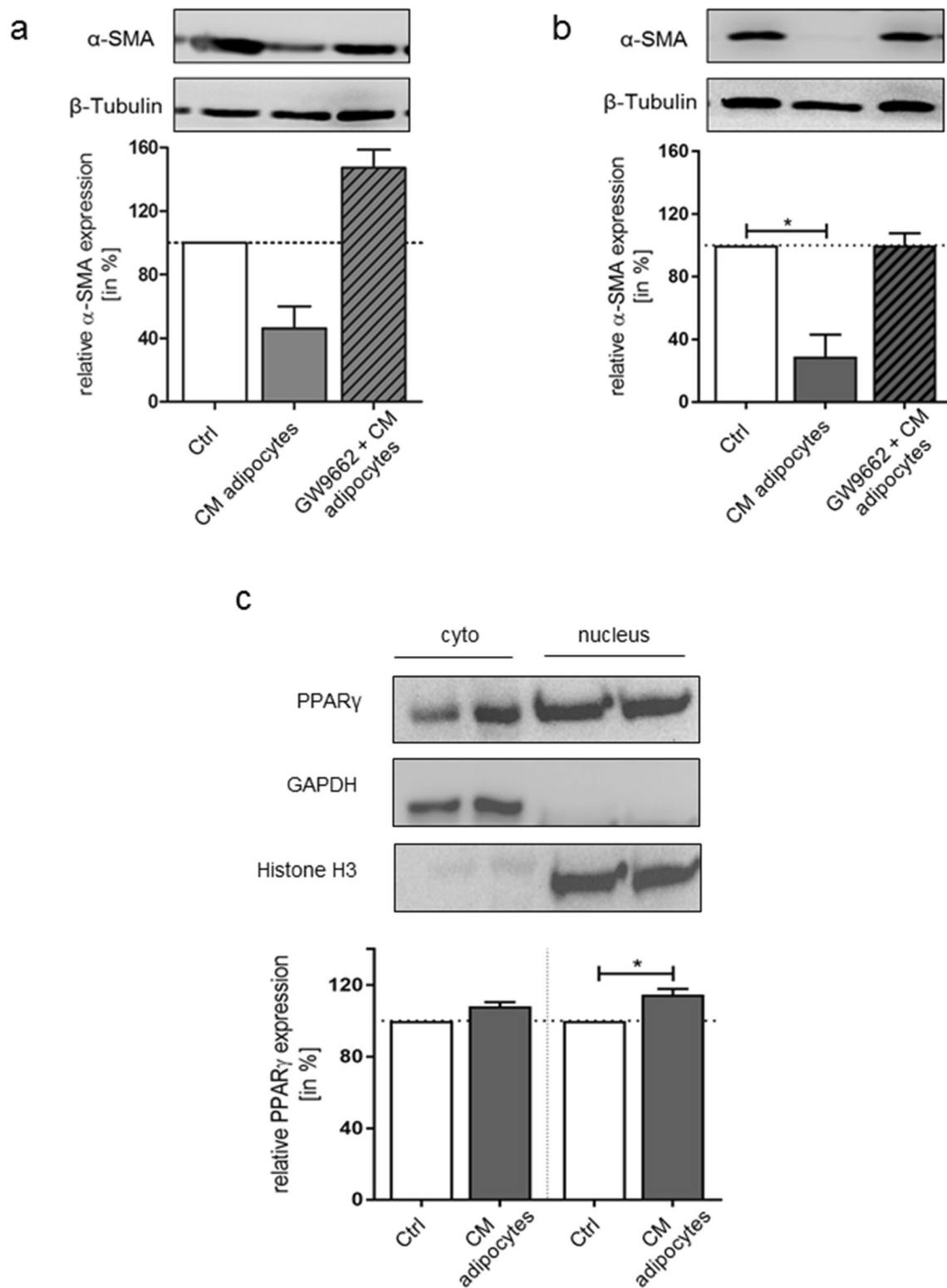


Fig. 4 Antagonizing PPAR γ abolishes the α -SMA reduction observed after exposure to adipocyte-CM. Representative Western blots and relative protein expression (semi-quantified via densitometry) of α -SMA in TGF- β -induced myofibroblasts (**a**) and hypertrophic scar fibroblasts (**b**) after preincubation with GW9662 followed by CM-treatment. β -Tubulin served as the loading control. **c** Representative Western blots and relative

protein expression (semi-quantified by densitometry) of peroxisomal proliferator-activated receptor γ (PPAR γ) after subfractionation of TGF- β -induced myofibroblasts. GAPDH served as the loading control for cytoplasmic fractions; Histone H3 for nuclear fractions. Ctrl = control, serum-free medium treatment. The data are presented as the mean \pm SEM; $n = 3$ ($*p \leq 0.05$)

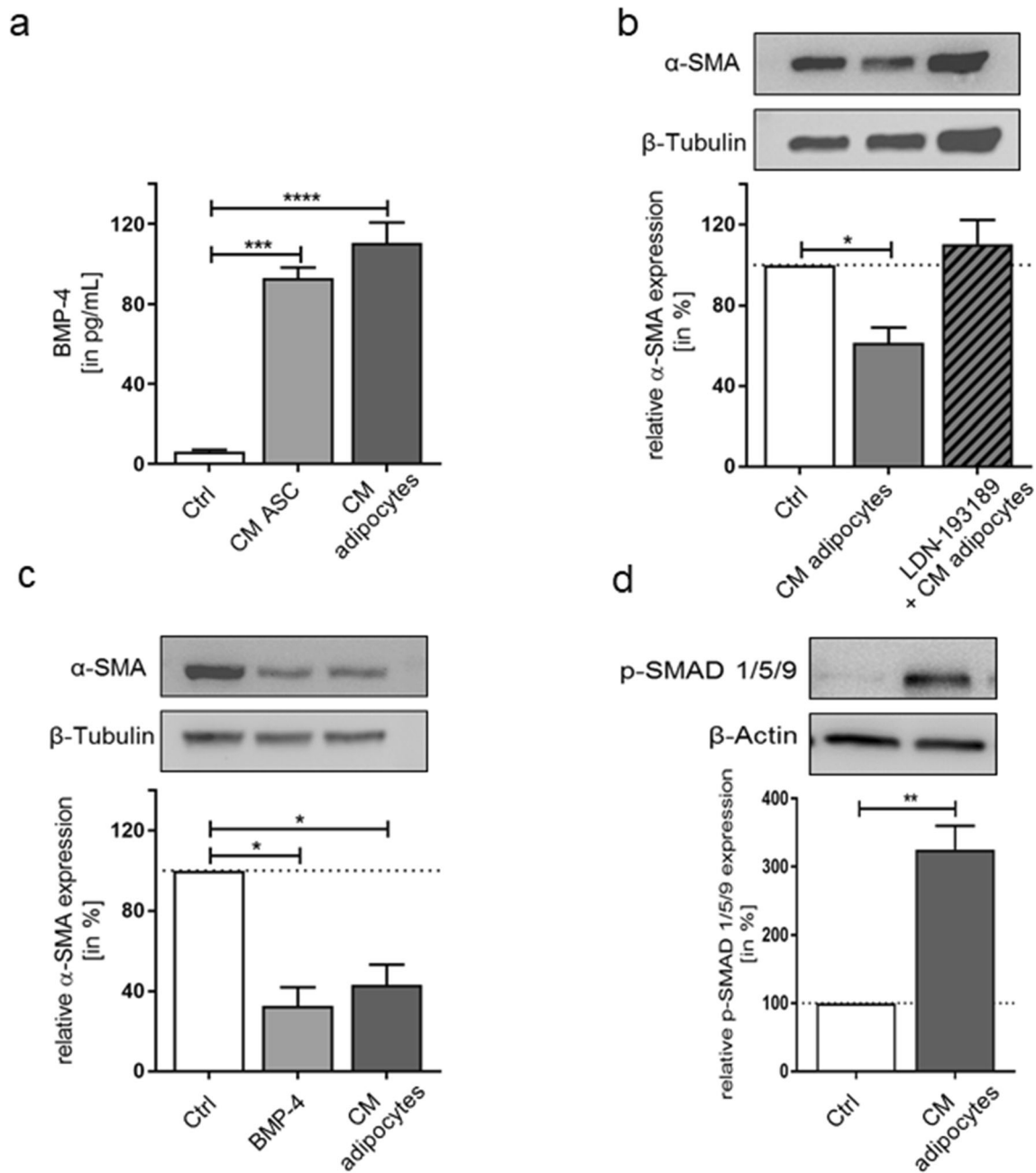


Fig. 5 BMP-4 is involved in myofibroblast reprogramming. **a** Bone morphogenetic protein (BMP)-4 secretion from adipocytes and adipose-derived stem cells (ASCs) measured by ELISA (Ctrl = control, serum-free DMEM/F12). **b** Representative Western blots of α -SMA expression following TGF- β -induced myofibroblast preincubation with the BMP receptor inhibitor LDN-193189 prior to incubation with adipocyte-CM. **c** α -SMA protein expression in TGF- β -induced myofibroblasts after

stimulation with 20 ng/mL recombinant BMP-4 or adipocyte-CM. **d** Representative Western blots of p-SMAD 1/5/9 expression in TGF- β -induced myofibroblasts following adipocyte-CM incubation. The relative protein expression of target proteins was semi-quantified by densitometry and compared with β -actin or β -tubulin expression. The data are presented as the mean \pm SEM; $n = 3-5$ (* $p \leq 0.05$; ** $p \leq 0.01$; *** $p \leq 0.001$; **** $p \leq 0.0001$)

was found (Fig. 3a, b). Again, adipocyte-CM induced a stronger downregulation compared with ASC-CM. Further analyses of non-canonical TGF- β effectors showed a significant reduction in phosphorylated p38 levels (Fig. 3c, d), whereas no changes were observed for stress-activated protein kinase/c-Jun NH2-terminal kinase (SAPK/JNK, Fig. S2B).

Antagonizing PPAR γ abolishes α -SMA reduction after exposure to adipocyte-CM

To unravel the impact of the nuclear receptor PPAR γ on α -SMA expression, myofibroblasts and fibroblasts from hypertrophic scars were preincubated with the PPAR γ antagonist GW9662 prior to exposure to CM. Interestingly,

preincubation with GW9662 completely abolished the α -SMA downregulation, initially triggered by CM, resulting in no statistically different α -SMA levels compared to the untreated control (Fig. 4 a, b). Furthermore, PPAR γ expression before and after TGF- β -induced myofibroblast exposure to adipocyte-CM was assessed by subfractionation, which showed an increased trend in PPAR γ expression by $8\% \pm 2.4\%$ in cytoplasmic extracts and significantly increased PPAR γ expression in nuclear fractions ($14.6\% \pm 3.3\%$) (Fig. 4c).

BMP-4 is pivotal for myofibroblast reprogramming

Since the involvement of bone morphogenetic protein (BMP)-4 and BMP-2 in myofibroblast reprogramming has been recently shown [6], BMP secretion by ASCs and adipocytes was analyzed via ELISA, and the results showed distinct levels of BMP-4 (Fig. 5a), whereas BMP-2, BMP-6, and BMP-7 were not detected. To further analyze the role of BMP-4, TGF- β -induced myofibroblasts were preincubated with the BMP receptor type I inhibitor LDN-193189, which abolished the effects of adipocyte-CM, resulting in unchanged α -SMA levels (Fig. 5b). To verify the involvement of BMP-4, 20 ng/mL recombinant human BMP-4 was added to TGF- β -induced myofibroblasts and led to distinct α -SMA downregulation comparable to that induced by incubation with adipocyte-CM (Fig. 5c). In addition, activation of BMP signaling, and hence the phosphorylation pattern of the SMAD 1/5/9 complex, was analyzed. As anticipated, the expression of phosphorylated SMAD 1/5/9 increased significantly in TGF- β -induced myofibroblasts following incubation with adipocyte-CM (Fig. 5d).

Incubation with BMP-4 and adipocyte-CM does not induce myofibroblast trans-differentiation

Recent studies have indicated the potential of BMP-4 to induce adipogenic transformation of scar fibroblasts *in vitro* and *in vivo* [6], and thus, myofibroblasts as well as fibroblasts from hypertrophic scars and keloids were stimulated with 20 ng/mL BMP-4 or adipocyte-CM for 48 h, followed by further cultivation in adipogenesis medium for another 10 days. No lipid droplet formation or significant increases in characteristic adipogenic genes or proteins were observed (Fig. S3).

High-throughput analysis of myofibroblast protein expression indicates distinct alterations in BMP and PPAR γ signaling following incubation with adipocyte-CM

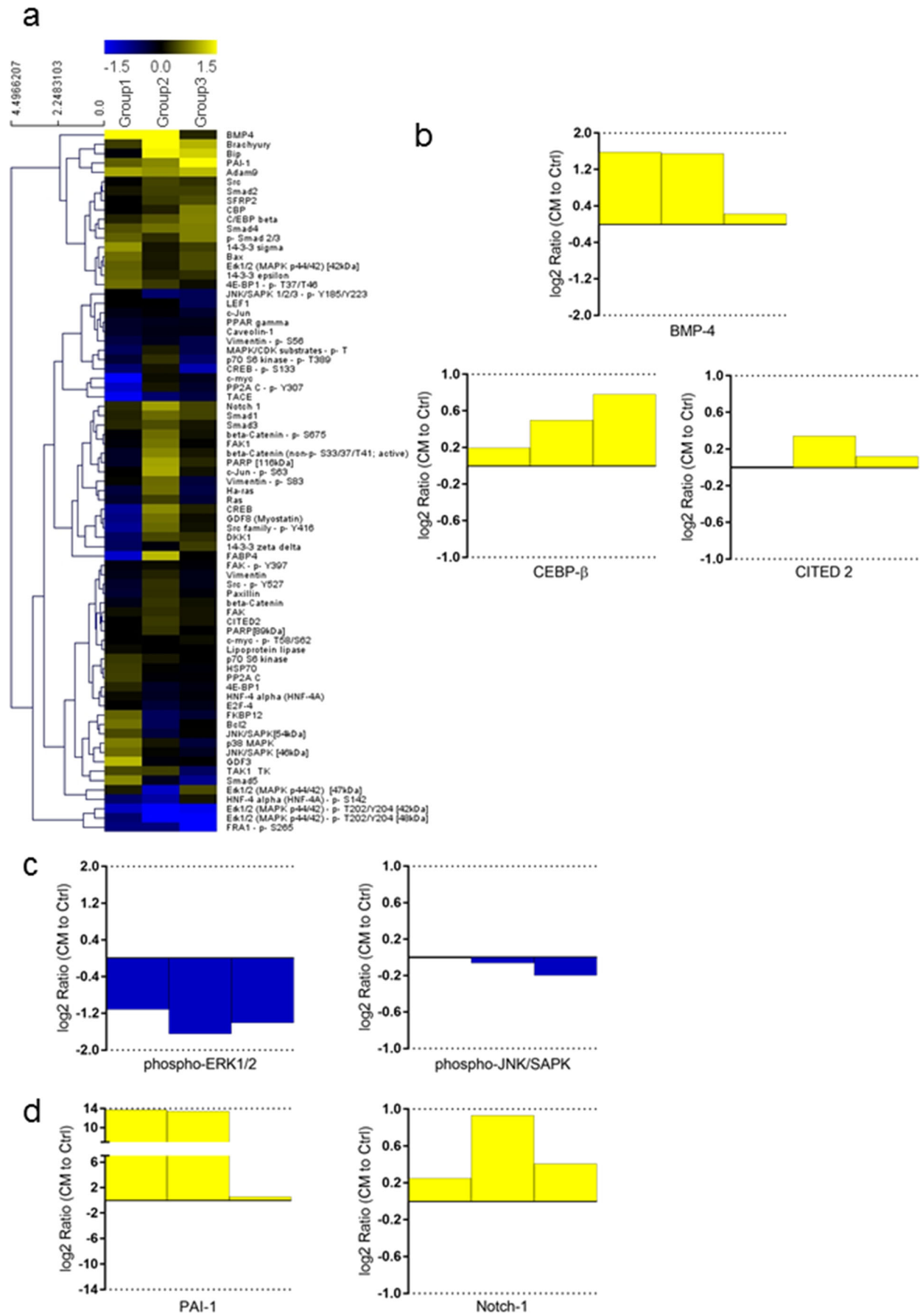
For a more comprehensive analysis of the effects of adipocyte-CM on TGF- β -induced myofibroblasts, bead-based DigiWest[®] analysis, a high-throughput Western blot

approach, was performed. Hierarchical clustering (HCL) analysis revealed up- (yellow) or downregulation (blue) of 77 proteins (Fig. 6a). However, it must be noted that donor variability needs to be considered. Two out of three pooled myofibroblast samples showed significantly increased BMP-4 protein expression after incubation with adipocyte-CM. Interestingly, the expression levels of the transcription factor CCAAT/enhancer-binding protein β (CEBP β) and transcriptional coactivator Cbp/P300-interacting transactivator with Glu/Asp rich carboxy-terminal domain 2 (CITED2), both of which are associated with PPAR γ activation, were enhanced (Fig. 6b). The expression of phosphorylated ERK 1/2 was consistently reduced in all samples (Fig. 6c), which confirms previous findings (Fig. 3a, b). HCL analysis further indicated alterations in Wnt signaling elements, although currently, no clear conclusion can be drawn because both inducers and inhibitors of Wnt pathways seemed to be modulated after myofibroblast incubation with adipocyte-CM. Notably, increased expression of plasminogen activator inhibitor (PAI)-1 and Notch-1 (Fig. 6d) were observed, both of which are associated with myofibroblast differentiation.

Discussion

Over the past years, new insights into the functionality and composition of adipose tissue have stimulated speculation about its regenerative potential. In this regard, adipose-derived stem cells (ASCs) have been investigated for the treatment of various conditions, including burn scars, ulcers, and breast reconstruction following mastectomy. Moreover, the beneficial effects of ASCs on wound healing as well as their anti-fibrotic effects have been reported [9, 10, 22]. In contrast, thus far, the regenerative potential of adipocytes has rarely been studied. In fact, only few studies have reported on the effects of adipocytes on wound healing. Among them, Schmidt and Horsley demonstrated that enhanced proliferation of adipocyte precursor cells and adipocyte repopulation in skin wounds after inflammation is crucial for adequate wound healing [23]. Moreover, the primary adipokines adiponectin and leptin seem to facilitate re-epithelialization [24, 25]. Recently, autologous fat grafting has increasingly been used,

Fig. 6 High-throughput analysis of myofibroblast protein expression indicates distinct alteration of BMP and PPAR γ signaling following incubation with adipocyte-CM. TGF- β -induced myofibroblast protein expression following adipocyte-CM stimulation was analyzed by the DigiWest[®] bead-based multiplex Western blot analysis. **a** For clustering, ratios were calculated between CM-treated and untreated samples from each group followed by log₂ transformation. Hierarchical clustering (HCL) was performed on the log₂ transformed ratios using MeV 4.9.0 software. Each group represents a pool of cells from three independent donors. See also Table S3. Protein expression levels of **b** CITED2, BMP-4, and CEBP β ; **c** p-ERK 1/2 and p-JNK/SAPK; **d** PAI-1 and Notch1 in the three analyzed groups



for example, as part of breast reconstruction following mastectomy, and has resulted in significant improvements in scar appearance and tissue functionality over time [26]. However, while the underlying mechanism is unknown, the involvement of the paracrine effects of adipocytes has been proposed.

Hence, to study the regenerative potential of adipocytes, the effects of *in vitro* differentiated adipocytes on myfibroblasts and on fibroblasts from hypertrophic scars and keloids were investigated. First, the secretome of adipocytes was determined using mass spectrometry shot gut proteomics approach. Notably, data derived from a secretome analysis require careful interpretation because the results strongly depend on the experimental setup [27]. Nevertheless, 90 out of the 288 identified proteins have been previously found in the adipocyte secretome. In-depth analysis related to GO terms revealed that 23 of the proteins were associated with wound healing and 5

were associated with regeneration (Fig. 1), including collagen types 1, 3, and 5 and TIMP1, fibulin 1, and fibronectin 1.

In an investigation of the paracrine effects of adipocytes on myfibroblasts, incubation of myfibroblasts with adipocyte-CM showed a significant reduction in the myfibroblast marker α -SMA as well as reduced expression of the ECM components collagen 1 and 3 (Fig. 2), indicating myfibroblast reprogramming or dedifferentiation. This effect was most pronounced in fibroblasts isolated from hypertrophic scars and superior to the effect of ASC-CM. For the latter, the regulatory effects on α -SMA expression have been previously demonstrated [28–30]. A curious point is that ASCs themselves do express high α -SMA levels which seems unaffected by adipocytes. Potential reasons such as “protective” mechanism remain elusive. Interestingly, our results indicate stronger effects mediated by adipocytes compared to ASCs potentially

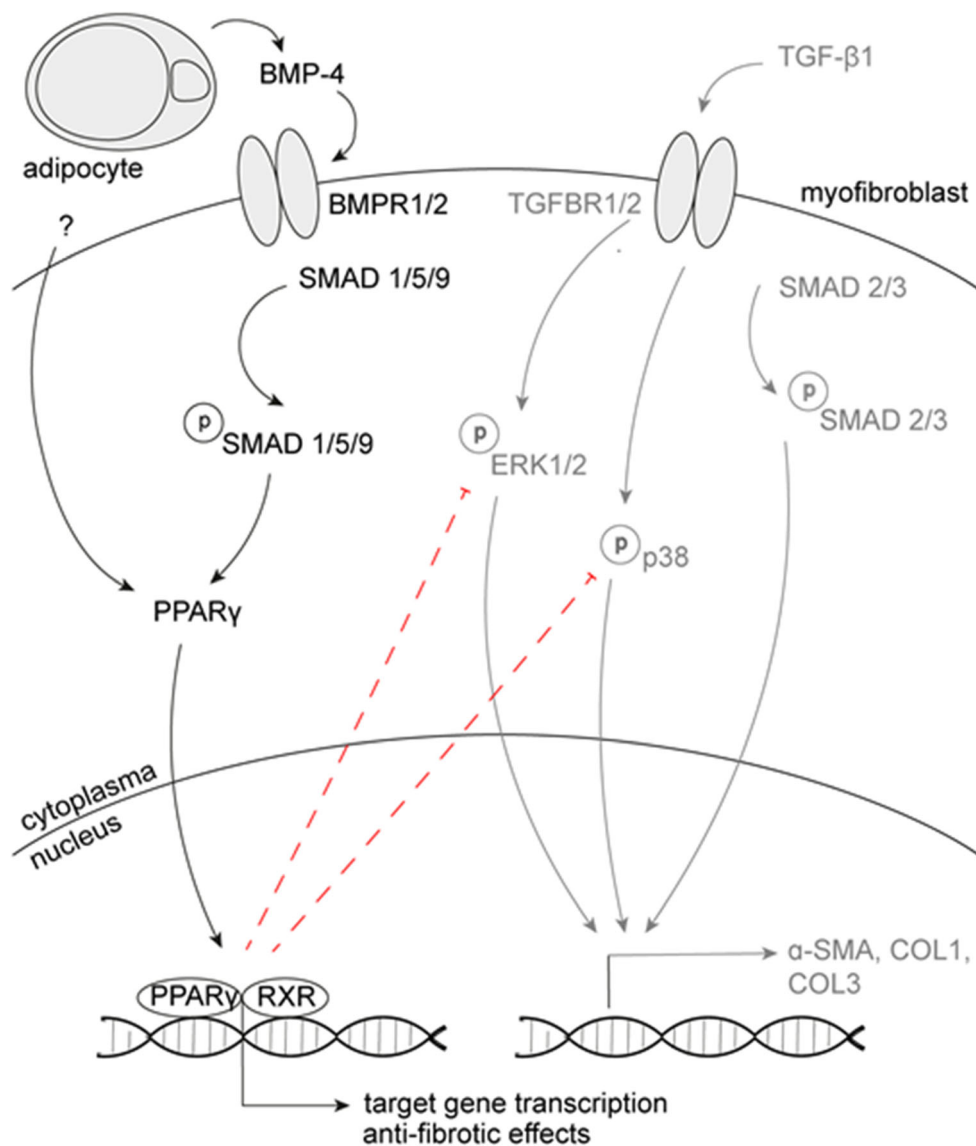


Fig. 7 Paracrine effectors secreted by adipocytes trigger myfibroblast reprogramming via BMP-4 secretion and PPAR γ activation. Schematic depiction of the cellular crosstalk between adipocytes and myfibroblasts

due to the highly complex secretome of adipocytes (Table S4). However, it has to be noted that we have been working with in vitro differentiated adipocytes and the effect of mature adipocytes should be addressed in the future.

The α -SMA reduction seems to be at least partially mediated by PPAR γ receptor activation because no α -SMA down-regulation was observed when PPAR γ was blocked (Fig. 4). Interestingly, previous studies have reported anti-fibrotic effects of PPAR γ induced by attenuation or even inhibition of TGF- β signaling [14, 31, 32]. Notably, reduced PPAR γ expression and enhanced TGF- β signaling is associated with progressive fibrogenesis [33]. The underlying mechanisms of the TGF- β -antagonizing effect of PPAR γ are the subject of our ongoing studies. Our data indicate the occurrence of SMAD-independent changes in TGF- β signaling because the MAPKs ERK and p38 exhibited reduced expression in adipocyte-CM-treated myofibroblasts and hypertrophic scar fibroblasts (Fig. 3). In addition, subfractionation of CM-treated myofibroblasts revealed increased PPAR γ expression in the cytoplasmic and nuclear fractions (Fig. 4). Interestingly, high-throughput protein analysis showed an upregulation of CITED2 in myofibroblasts after incubation with adipocyte-CM (Fig. 6). CITED2 is a transcriptional activator for both TGF- β and PPAR γ [34, 35], and it may be speculated that both TGF- β -dependent SMADs and PPAR γ compete for the same pool of CITED2 molecules for efficient target gene activation. Altogether, these results indicate that direct as well as indirect activation of PPAR γ signaling shifts the balance toward anti-fibrotic effects. However, thus far, the component of adipocyte-CM that directly activates PPAR γ receptor is unknown.

Although the decreased expression levels of α -SMA and collagen 1 and 3 indicate a dedifferentiation of myofibroblasts, their specific fate remains to be elucidated, which is challenging because specific markers to characterize and distinguish myofibroblasts and fibroblasts have not yet been identified. A recent study from Plikus et al. reported myofibroblast reprogramming into the adipogenic lineage induced by BMP-2 and BMP-4 secreted from hair follicles during wound healing in mice [6]. Concordant results were obtained from in vitro assays with stimulated keloid fibroblasts. Notably, in our study, BMP-4 was secreted by adipocytes (Fig. 5), and inhibition of BMP receptor type I abolished the reduction in α -SMA expression in myofibroblasts, indicating an involvement of BMP-4 in myofibroblast reprogramming (Fig. 5). Moreover, DigiWest[®] analysis showed enhanced BMP-4 protein expression in myofibroblasts following stimulation with adipocyte-CM (Fig. 6), which is in line with recent findings in human esophageal myofibroblasts [36]. Members of the BMP family, especially BMP-2, BMP-4, and BMP-7, are known for their anti-fibrotic potential by opposing the actions of TGF- β signaling [37–39].

However, in contrast with Plikus et al., we were not able to induce adipogenic differentiation of hypertrophic scar or

keloid fibroblasts (Fig. S3). Moreover, high-throughput protein analysis provided evidence that myofibroblast characteristics are still present, as indicated by the high expression levels of PAI-1 or Notch-1 (Fig. 6), which are both strongly associated with fibrosis [40]. The contradictory findings may result from differences in the composition of the adipogenesis medium. Nevertheless, some data may indicate the onset of adipogenic differentiation because increased CEBP β expression and activation of BMP-4/SMAD 1/5/9-signaling, both of which are key activators of adipogenesis, were found in myofibroblasts after incubation with adipocyte-CM (Figs. 5 and 6; S3). This result is in line with recent data demonstrating enhanced expression of PPAR γ in 3T3-L1 adipocytes [41] and differentiation of precursor cells into the adipocyte lineage [42, 43] after incubation with BMPs. However, further studies are necessary to draw final conclusions.

In conclusion, our data indicate that adipocytes can induce myofibroblast reprogramming. These paracrine effects are mediated by direct and indirect activation of PPAR γ signaling as well as by the release of BMP-4 and subsequent stimulation of BMP signal transduction; both of these signaling pathways are known for their TGF- β -antagonizing and hence anti-fibrotic effects (Fig. 7). These data demonstrate the regenerative potential of adipocytes and provide new insights into the regenerative processes triggered by autologous fat grafting. A more detailed understanding of these mechanisms may pave the way toward novel strategies for scar prevention or treatment. Nevertheless, it remains open to what extent other cell types of the stromal vascular fraction (SVF) such as pericytes, endothelial cells, macrophages etc. residing in the autologous fat grafts may also contribute to myofibroblast dedifferentiation. This requires specific attention since BMP-4 production, for example, has been recently shown in endothelial cells [44]. However, these aspects were beyond the focus of the current work but clearly require further attention in future investigations.

Acknowledgments The authors thank Patrick Graff and Maria Thon for technical assistance. Moreover, the authors would like to acknowledge the support of Anja Briese and Dr. Christoph Sachse (NMI TT Pharmaservices).

Author contributions K.H., G.E., and O.K. performed experiments. S.H., L.v.B. (at VUmc), and S.G. (at VUmc) supervised the work. K.H. and S.H. designed the experiments, analyzed the data, and wrote the manuscript. All the authors provided critical review of the manuscript.

Funding information This work was financially supported by the Einstein Center for Regenerative Therapies (ECRTs) and the Berlin-Brandenburg School for Regenerative Therapies (BSRT).

Compliance with ethical standards

Conflict of interest The authors declare that they have no conflict of interest.

References

- Mokos ZB, Jovic A, Grgurevic L, Dumic-Cule I, Kostovic K, Ceovic R, Marinovic B (2017) Current therapeutic approach to hypertrophic scars. *Front Med (Lausanne)* 4:83
- Hinz B (2016) The role of myofibroblasts in wound healing. *Curr Res Transl Med* 64(4):171–177
- Sarrazy V, Billet F, Micallef L, Coulomb B, Desmouliere A (2011) Mechanisms of pathological scarring: role of myofibroblasts and current developments. *Wound Repair Regen* 19(Suppl 1):s10–s15
- Hecker L, Jagirdar R, Jin T, Thannickal VJ (2011) Reversible differentiation of myofibroblasts by MyoD. *Exp Cell Res* 317(13):1914–1921
- Garrison G, Huang SK, Okunishi K, Scott JP, Kumar Penke LR, Scruggs AM, Peters-Golden M (2013) Reversal of myofibroblast differentiation by prostaglandin E(2). *Am J Respir Cell Mol Biol* 48(5):550–558
- Plikus MV, Guerrero-Juarez CF, Ito M, Li YR, Dedhia PH, Zheng Y, Shao M, Gay DL, Ramos R, Hsi TC et al (2017) Regeneration of fat cells from myofibroblasts during wound healing. *Science* 355(6326):748–752
- Klinger M, Marazzi M, Vigo D, Torre M (2008) Fat injection for cases of severe burn outcomes: a new perspective of scar remodeling and reduction. *Aesthet Plast Surg* 32(3):465–469
- Zuk PA, Zhu M, Ashjian P, De Ugarte DA, Huang JJ, Mizuno H, Alfonso ZC, Fraser JK, Benhaim P, Hedrick MH (2002) Human adipose tissue is a source of multipotent stem cells. *Mol Biol Cell* 13(12):4279–4295
- Kim WS, Park BS, Sung JH, Yang JM, Park SB, Kwak SJ, Park JS (2007) Wound healing effect of adipose-derived stem cells: a critical role of secretory factors on human dermal fibroblasts. *J Dermatol Sci* 48(1):15–24
- Zhang Q, Liu LN, Yong Q, Deng JC, Cao WG (2015) Intralesional injection of adipose-derived stem cells reduces hypertrophic scarring in a rabbit ear model. *Stem Cell Res Ther* 6:145
- Rosen ED, Spiegelman BM (2006) Adipocytes as regulators of energy balance and glucose homeostasis. *Nature* 444(7121):847–853
- Kim EY, Kim WK, Oh KJ, Han BS, Lee SC, Bae KH (2015) Recent advances in proteomic studies of adipose tissues and adipocytes. *Int J Mol Sci* 16(3):4581–4599
- Lehrke M, Lazar MA (2005) The many faces of PPARgamma. *Cell* 123(6):993–999
- Ghosh AK, Bhattacharyya S, Lakos G, Chen SJ, Mori Y, Varga J (2004) Disruption of transforming growth factor beta signaling and profibrotic responses in normal skin fibroblasts by peroxisome proliferator-activated receptor gamma. *Arthritis Rheum* 50(4):1305–1318
- Zheng F, Fomoni A, Elliot SJ, Guan Y, Breyer MD, Striker LJ, Striker GE (2002) Upregulation of type I collagen by TGF- β in mesangial cells is blocked by PPAR γ activation. *Am J Physiol Renal Physiol* 282(4):F639–F648
- Treindl F, Ruprecht B, Beiter Y, Schultz S, Döttinger A, Staebler A, Joos TO, Kling S, Poetz O, Fehm T (2016) A bead-based western for high-throughput cellular signal transduction analyses. *Nat Commun* 7:12852
- Becker M, Maring JA, Schneider M, Herrera Martin AX, Seifert M, Klein O, Braun T, Falk V, Stamm C (2018) Towards a novel patch material for cardiac applications: tissue-specific extracellular matrix introduces essential key features to decellularized amniotic membrane. *Int J Mol Sci* 19(4):1032
- Ojima K, Oe M, Nakajima I, Muroya S, Nishimura T (2016) Dynamics of protein secretion during adipocyte differentiation. *FEBS Open Bio* 6(8):816–826
- Zvonic S, Lefevre M, Kilroy G, Floyd ZE, DeLany JP, Kheterpal I, Gravois A, Dow R, White A, Wu X et al (2007) Secretome of primary cultures of human adipose-derived stem cells: modulation of serpins by adipogenesis. *Mol Cell Proteomics* 6(1):18–28
- Alvarez-Llamas G, Szalowska E, de Vries MP, Weening D, Landman K, Hoek A, Wolffebuttel BHR, Roelofsens H, Vonk RJ (2007) Characterization of the human visceral adipose tissue secretome. *Mol Cell Proteomics* 6(4):589–600
- Zhong J, Krawczyk SA, Chaerkady R, Huang H, Goel R, Bader JS, Wong GW, Corkey BE, Pandey A (2010) Temporal profiling of the secretome during adipogenesis in humans. *J Proteome Res* 9(10):5228–5238
- Schaffler A, Buchler C (2007) Concise review: adipose tissue-derived stromal cells—basic and clinical implications for novel cell-based therapies. *Stem Cells* 25(4):818–827
- Schmidt BA, Horsley V (2013) Intradermal adipocytes mediate fibroblast recruitment during skin wound healing. *Development* 140(7):1517–1527
- Salathia NS, Shi J, Zhang J, Glynne RJ (2013) An in vivo screen of secreted proteins identifies adiponectin as a regulator of murine cutaneous wound healing. *J Invest Dermatol* 133(3):812–821
- Frank S, Stallmeyer B, Kämpfer H, Kolb N, Pfeilschifter J (2000) Leptin enhances wound re-epithelialization and constitutes a direct function of leptin in skin repair. *J Clin Invest* 106(4):501–509
- Klinger M, Caviggioli F, Klinger FM, Giannasi S, Bandi V, Banzatti B, Forcellini D, Maione L, Catania B, Vinci V (2013) Autologous fat graft in scar treatment. *J Craniofac Surg* 24(5):1610–1615
- Chevallet M, Diemer H, Van Dorssealer A, Villiers C, Rabilloud T (2007) Toward a better analysis of secreted proteins: the example of the myeloid cells secretome. *Proteomics* 7(11):1757–1770
- Spiekman M, Przybyt E, Plantinga JA, Gibbs S, van der Lei B, Harmsen MC (2014) Adipose tissue-derived stromal cells inhibit TGF- β 1-induced differentiation of human dermal fibroblasts and keloid scar-derived fibroblasts in a paracrine fashion. *Plast Reconstr Surg* 134(4):699–712
- Verhoekx JS, Mudera V, Walbeehm ET, Hovius SE (2013) Adipose-derived stem cells inhibit the contractile myofibroblast in Dupuytren's disease. *Plast Reconstr Surg* 132(5):1139–1148
- Li Y, Zhang W, Gao J, Liu J, Wang H, Li J, Yang X, He T, Guan H, Zheng Z et al (2016) Adipose tissue-derived stem cells suppress hypertrophic scar fibrosis via the p38/MAPK signaling pathway. *Stem Cell Res Ther* 7(1):102
- Burgess HA, Daugherty LE, Thatcher TH, Lakatos HF, Ray DM, Redonnet M, Phipps RP, Sime PJ (2005) PPARgamma agonists inhibit TGF-beta induced pulmonary myofibroblast differentiation and collagen production: implications for therapy of lung fibrosis. *Am J Physiol Lung Cell Mol Physiol* 288(6):L1146–L1153
- Aoki Y, Maeno T, Aoyagi K, Ueno M, Aoki F, Aoki N, Nakagawa J, Sando Y, Shimizu Y, Suga T et al (2009) Pioglitazone, a peroxisome proliferator-activated receptor gamma ligand, suppresses bleomycin-induced acute lung injury and fibrosis. *Respiration* 77(3):311–319
- Wei J, Ghosh AK, Sargent JL, Komura K, Wu M, Huang QQ, Jain M, Whitfield ML, Feghali-Bostwick C, Varga J (2010) PPARgamma downregulation by TGFss in fibroblast and impaired expression and function in systemic sclerosis: a novel mechanism for progressive fibrogenesis. *PLoS One* 5(11):e13778
- Chou YT, Wang H, Chen Y, Danielpour D, Yang YC (2006) Cited2 modulates TGF-beta-mediated upregulation of MMP9. *Oncogene* 25(40):5547–5560
- Tien ES, Davis JW, Vanden Heuvel JP (2004) Identification of the CREB-binding protein/p300-interacting protein CITED2 as a peroxisome proliferator-activated receptor alpha coregulator. *J Biol Chem* 279(23):24053–24063

36. Zhang C, Niu C, Yang K, Shaker A (2018) Human esophageal myofibroblast secretion of bone morphogenetic proteins and GREMLIN1 and paracrine regulation of squamous epithelial growth. *Sci Rep* 8(1):12354
37. McVicker BL, Bennett RG (2017) Novel anti-fibrotic therapies. *Front Pharmacol* 8:318
38. Shlyonsky V, Soussia IB, Naeije R, Mies F (2011) Opposing effects of bone morphogenetic protein-2 and endothelin-1 on lung fibroblast chloride currents. *Am J Respir Cell Mol Biol* 45(6):1154–1160
39. Pegorier S, Campbell GA, Kay AB, Lloyd CM (2010) Bone morphogenetic protein (BMP)-4 and BMP-7 regulate differentially transforming growth factor (TGF)-beta1 in normal human lung fibroblasts (NHLF). *Respir Res* 11:85
40. Ghosh AK, Vaughan DE (2012) PAI-1 in tissue fibrosis. *J Cell Physiol* 227(2):493–507
41. Schreiber I, Dorpholz G, Ott CE, Kragesteen B, Schanze N, Lee CT, Kohrle J, Mundlos S, Ruschke K, Knaus P (2017) BMPs as new insulin sensitizers: enhanced glucose uptake in mature 3T3-L1 adipocytes via PPARgamma and GLUT4 upregulation. *Sci Rep* 7(1):17192
42. Huang H, Song T-J, Li X, Hu L, He Q, Liu M, Lane MD, Tang Q-Q (2009) BMP signaling pathway is required for commitment of C3H10T1/2 pluripotent stem cells to the adipocyte lineage. *Proc Natl Acad Sci* 106(31):12670–12675
43. Hammarstedt A, Hedjazifar S, Jenndahl L, Gogg S, Grunberg J, Gustafson B, Klimcakova E, Stich V, Langin D, Laakso M et al (2013) WISP2 regulates preadipocyte commitment and PPARgamma activation by BMP4. *Proc Natl Acad Sci U S A* 110(7):2563–2568
44. Wertheimer T, Velardi E, Tsai J, Cooper K, Xiao S, Kloss CC, Ottmuller KJ, Mokhtari Z, Brede C, deRoos P et al (2018) Production of BMP4 by endothelial cells is crucial for endogenous thymic regeneration. *Sci Immunol* 3(19); doi: 10.1126/sciimmunol.aal2736

Publisher's note Springer Nature remains neutral with regard to jurisdictional claims in published maps and institutional affiliations.